Available online at www.sciencedirect.com
SCIENCE DIRECT
Polymer 47 (2006) 6117–6122
polymer
www.elsevier.com/locate/polymer

Vapor sorption in thin supported polymer films studied by white light interferometry

Kyriaki Manoli [a,b], Dimitris Goustouridis [a], Stavros Chatzandroulis [a], Ioannis Raptis [a], Evangelos S. Valamontes [c], Merope Sanopoulou [b,*]

[a] *Institute of Microelectronics, NCSR ''Demokritos'', 15310 Ag. Paraskevi Attikis, Athens, Greece*
[b] *Institute of Physical Chemistry, NCSR ''Demokritos'', 15310 Ag. Paraskevi Attikis, Athens, Greece*
[c] *Department of Electronics, Technological Educational Institute of Athens, 12210 Aegaleo, Greece*

Received 20 April 2006; received in revised form 30 May 2006; accepted 9 June 2006
Available online 7 July 2006

Abstract

In the present study, we apply a white light interferometric methodology to study sorption of moisture and methanol vapor in thin films of poly(2-hydroxyethyl methacrylate) [PHEMA] and poly(methyl methacrylate) [PMMA], supported on oxidized silicon wafers. The measured equilibrium thickness expansion of each film, exposed to different activities of the vapor penetrant, is used to determine the sorption isotherm of the system. Results for relatively thick films (100 nm $< L_o <$ 600 nm) are compared with corresponding literature data for bulk, free-standing films, obtained by direct gravimetric methods. Furthermore, PMMA films of thicknesses lower than 100 nm were employed in order to study the effect of the dry film's thickness, and of substrate, on fractional swelling.

Keywords: Vapor sorption; Poly(2-hydroxyethyl methacrylate); Poly(methyl methacrylate)

1. Introduction

Moisture and organic vapor sorption in, and concurrent swelling of, ultrathin supported polymer films is important in many applications, such as coatings, microelectronics manufacturing and chemical sensors (e.g. [1,2]). Conventional gravimetric methods are not always suitable for studying these phenomena in ultrathin supported films. Accordingly, various techniques have been applied, such as quartz crystal microbalance for mass uptake measurements [1,3–5] and specular X-ray reflectivity [1,4,6–8], ellipsometry [9,10], or interferometry [11] for monitoring thickness changes due to sorption. The latter type of measurements is also used to estimate mass or volume fraction of the sorbed penetrant, assuming unidirectional swelling due to the constraining rigid support [1,4,6,7,9–11]. In certain cases the sorption isotherms deduced by the application of the above techniques in supported films have been compared with the corresponding data deduced by conventional methods in free-standing, bulk films. The results indicate that the former type of films may sorb differently from the latter [9–11]. Moreover, studies on ultrathin supported films of different thicknesses L_o (<100 nm), mainly focused on moisture absorption, indicate that equilibrium fractional swelling, due to exposure to a constant vapor activity, is thickness-dependent [1,3,4,6–8]. For relatively hydrophobic poly(4-*tert*-butoxycarbonyloxystyrene) films supported on hydrophilic SiO_2 substrate, an enhancement of fractional swelling with decreasing film thickness was observed [6]. A similar, although weaker, effect was observed for the same polymer supported on Al_2O_3 [7] as well as for a polyimide supported on SiO_2 [8]. This behavior was attributed to the accumulation of excess water near the polymer–hydrophilic substrate interface, and the interpretation was supported by water distribution profiles determined by specular neutron reflectivity measurements [6,7]. Furthermore, treatment of the Al_2O_3 substrate surface with a hydrophobic

* Corresponding author. Tel.: +30 210 6503785; fax: +30 210 6511766.
E-mail address: sanopoul@chem.demokritos.gr (M. Sanopoulou).

0032-3861/$ - see front matter © 2006 Elsevier Ltd. All rights reserved.
doi:10.1016/j.polymer.2006.06.016

agent reduced the degree of interfacial water at the buried interface [7]. In general, the water concentration profile near the substrate is thought to depend on the relative hydrophobicity (hydrophilicity) of the polymer and substrate. Thus, fractional swelling of hydrophilic poly(vinyl pyrrolidone) supported on SiO_2 was found to be independent of thickness, while treatment of the SiO_2 surface with hydrophobic hexamethyldisilizane (HMDS) resulted in decreasing fractional swelling with decreasing film thickness [4].

Other physical properties of ultrathin supported films, such as diffusivity and glass transition temperature, have also been found to differ from those of the bulk, due to the significant contribution of interfacial effects to the properties of the film, when the latter's dimensions approach the radius of gyration of the polymer's molecule. For example, the glass transition temperature of ultrathin PMMA films was found to increase with decreasing film thickness for films supported on silicon dioxide substrate [12–14]. In contrast, the T_g of PMMA films supported on gold [13] or silicon dioxide treated with HMDS [12] substrates was found to decrease with decreasing film thickness. In the case of polystyrene, the T_g of supported films [15] (as well the solvent-induced T_g of polymer brushes [16]) has also been found to be thickness-dependent. Although these phenomena are not completely clarified, the prevailing interpretation is based on the concept that a supported film consists of three layers [15,17]. The polymer layer near the free surface (polymer–air interface) is characterized by enhanced mobility and reduced packing density as compared to the bulk polymer. The middle layer behaves like bulk polymer. The properties of the layer near the solid substrate depend on the strength of polymer–substrate interactions. As the film thickness decreases, the contribution of the top and bottom layers becomes increasingly significant and determines the thickness dependence of the apparent T_g of the film. Thus, in the case of strong polymer–substrate interactions, leading to restricted chain mobility in the layer near the solid substrate, the properties of this layer are the determinant factor and the T_g of the film increases with decreasing thickness. On the other hand, in the case of weak polymer–substrate interactions the free surface effect dominates, and T_g decreases with decreasing thickness. In line with the three layer model are molecular simulation studies [18] showing that, for dimensions lower than 30σ (where σ is the monomer diameter), free-standing films exhibit a decrease in the T_g with decreasing thickness, but the behavior of supported films depends on polymer–substrate interactions. In particular, T_g decreased with decreasing thickness for a weakly attractive substrate (having the same interaction strength parameters as the polymer), but the extent of reduction was less than that of the simulated free-standing film. In contrast, an increase in T_g was found for a strongly attractive substrate (having a polymer–surface interaction strength twice as that between polymer segments).

In the present work we apply a white light interferometric methodology to characterize the swelling behavior of thin supported films due to the sorption of methanol and water from the vapor phase. Films prepared from two polymers of different hydrophilicities are used: poly(2-hydroxyethyl methacrylate) [PHEMA] and poly(methyl methacrylate) [PMMA]. Data on the thickness expansion of relatively thick polymer films ($100\ \text{nm} < L_o < 600\ \text{nm}$), upon exposure to various activities of moisture and methanol vapor, are used to estimate the sorption isotherm of the system. Results are then compared with corresponding literature data obtained by direct gravimetric methods for bulk, free-standing films. Furthermore, PMMA films of thicknesses lower than 100 nm were employed in order to study the effect of the dry film's thickness, and of substrate, on fractional swelling.

2. Experimental

PMMA (MW ~ 120,000; density: 1.188 g/ml at 25 °C) and PHEMA (MW ~ 300,000; density: 1.15 g/ml at 25 °C) in the form of powder were purchased from Sigma–Aldrich. The radius of gyration R_g of each polymer's molecule was estimated, by group contribution methods [19], to be 8.7 and 14.8 nm for PMMA and PHEMA, respectively. Propylene glycol methyl ether acetate (PGMEA), ethyl lactate and methanol (MeOH) were also purchased from Sigma–Aldrich and used without further purification.

Polymer films, supported on oxidized silicon wafers, were prepared by spin-coating from 0.5–8% w/w solutions of PMMA in PGMEA, and of PHEMA in ethyl lactate. In certain experiments, partial hydrophobization of the support was effected by deposition, via spin-coating, of a few nanometers thick HMDS layer on the SiO_2 surface. The measured contact angles of water on bare, and HMDS-treated Si/SiO_2 substrate were $39 \pm 1^\circ$ and $67 \pm 2^\circ$, respectively. All supported films were heated on a hot plate for 15 min to 160 °C (PMMA) or 120 °C (PHEMA), in order to remove residual solvent and then were stored in a desiccator until further use. Dry film thicknesses L_o in the range 25–600 nm were used, corresponding to a range of $3–69R_g$ for PMMA and $2–40R_g$ for PHEMA.

For the measurement of changes in polymeric film thickness due to absorption/desorption of vapors, a home-made experimental set-up [20] has been used, consisting of the following sub-systems (i) a white light interferometry unit, (ii) a delivering sub-system for controlled concentrations of the vapor penetrant, (iii) a temperature controlled measuring chamber and (iv) a PC for the control of the sub-systems, and the data acquisition and processing.

The main parts of the white light interferometry unit are a light source, a spectrophotometer and a bifurcated optical fiber. A splitter optical fiber is connected to a vis–NIR light source (Avantes AvaLight HAL Tungsten-Halogen) through SMA connectors. The delivered optical power is equally divided into two beams: one directed to the slave channel of a PC driven double spectrophotometer, with a resolution of approximately 0.4 nm (Ocean Optics USB SD2000), and another connected to a bifurcated optical fiber. The outer part of the bifurcated optical fiber guides the light vertically onto the supported polymer film. The support is a Si wafer covered with a thermally grown, at 110 °C for 200 min, silicon dioxide layer of a final thickness of 1060 nm. Both the SiO_2 and the polymer used are transparent in the vis–NIR spectrum and

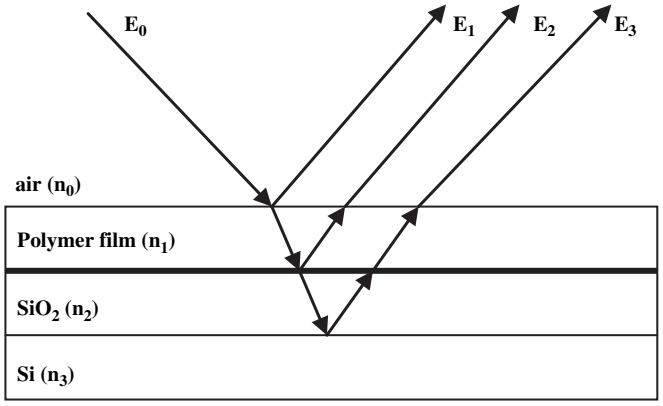

Fig. 1. Schematic presentation of interferometry principle.

thus, multiple reflections at the interfaces take place (Fig. 1) causing the interference signal. The total reflected beam is collected from the central part of the bifurcated optical fiber and is directed to the master channel of the spectrophotometer.

At each wavelength interference takes place, due to the light traveling through the transparent layers, and the final spectrum is recorded in the PC every 2 s. Film thickness changes, due to vapor penetrant absorption/desorption in the polymer layer, are monitored as changes in the recorded interference spectrum. The SiO_2 layer serves to increase the number of interference fringes in the recorded spectrum (by increasing the optical path of the traveling light) and thus, to improve significantly the fitting accuracy. The transparent layer was chosen to be from SiO_2 due to the process simplicity for its growth and the surface properties' stability over time. The presence of the SiO_2 layer, or any other transparent film, is necessary in the case of thin polymeric films (<200 nm thick). For considerably thicker polymeric films, e.g. 600 nm the intermediate layer is not required since the polymer film thickness provides long enough optical path which results in a sufficient number of spectrum extremums.

The total incident energy E on the spectrometer (Fig. 1), for each wavelength, can be approximated [21] by:

$$E = A + B\cos\left(\frac{4\pi n_1}{\lambda}L_1\right) + C\cos\left(\frac{4\pi n_2}{\lambda}L_2\right) + D\cos\left(\frac{4\pi n_2 L_2 + n_1 L_1}{\lambda}\right) \quad (1)$$

where

$$A = r_{01}^2 + r_{12}^2\left(1 - r_{01}^2\right)^2 + r_{23}^2\left(1 - r_{01}^2\right)^2\left(1 - r_{12}^2\right)^2$$

$$B = 2r_{01}r_{12}\left(1 - r_{01}^2\right)^2$$

$$C = 2r_{12}r_{23}\left(1 - r_{01}^2\right)\left(1 - r_{12}^2\right)^2$$

$$D = 2r_{01}r_{23}\left(1 - r_{01}^2\right)\left(1 - r_{12}^2\right)^2$$

$$r_{ij} = \frac{n_i - n_j}{n_i + n_j}$$

where n_i is the refractive index of the ith layer ($i = 0$ for air, 1 for the polymeric film, 2 for the SiO_2 layer and 3 for the Si substrate), L_1, L_2 the thicknesses of the polymeric film and the silicon dioxide, respectively, and λ the corresponding wavelength. The refractive indexes n_i of all layers vs wavelength are calculated with a spectroscopic ellipsometer (J.A. Wooks) and fitted to a three parameter (A, B, C) Cauchy model. By applying Eq. (1) for all wavelengths in the 470–740 nm spectrum range, the film thickness may be calculated for each recorded spectrum. The refractive index n_1 is assumed constant during the absorption/desorption of the vapor penetrant. This assumption leads to a small underestimation of the film thickness. As shown in the example of Fig. 2, the fitting accuracy is very high. The calculation time, for the fitting of the recorded spectrum with Eq. (1), is relatively small typically less than 500 ms and thus, it is possible to calculate in situ the polymeric film thickness changes.

The whole apparatus is controlled through a custom software developed under the LabView software platform.

For an absorption–swelling experiment, the supported polymer sample is placed in a thermostated chamber of ~150 ml volume. The desired penetrant activity a_s, is generated by mixing nitrogen with saturated penetrant vapor at 30 °C and at atmospheric pressure, and the mixture passes at a rate of 1000 ml/min (controlled by mass flow controllers) through the chamber containing the film, with its upper surface exposed to the stream. With the particular mass flow controllers used, the lowest activities attained in this study were 0.025 for methanol and 0.1 for moisture. After equilibrium swelling is achieved, desorption–contraction is effected by passing pure N_2 through the chamber. All experiments were performed at 30 ± 0.5 °C.

Each dry film of thickness L_o, when placed in the sorption chamber, was first heated to 120 °C in order to achieve the same thermal history for all the samples. After gradual cooling to 30 °C, the film was subjected to a series of absorption runs involving successive equilibration with progressively higher vapor activities a_s (= p/p_{sat}, where p_{sat} is the saturation pressure of the vapor at 30 °C), with intervening desorption steps back

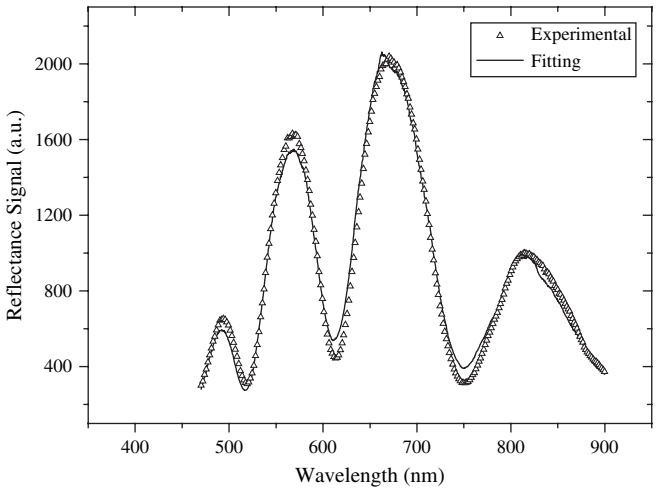

Fig. 2. Experimental spectrum (Δ) and theoretical fitting (−) of a dry PMMA film, supported on Si/SiO_2 substrate, exposed to pure nitrogen flow.

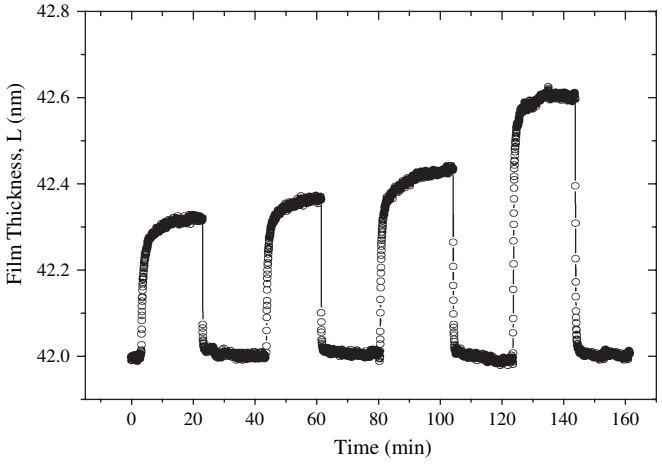

Fig. 3. Typical thickness expansion–contraction curves obtained when an initially dry, supported polymer film is subjected to a series of absorption runs involving successive equilibration with progressively higher vapor activities a_s, with intervening desorption steps back to $a_s = 0$.

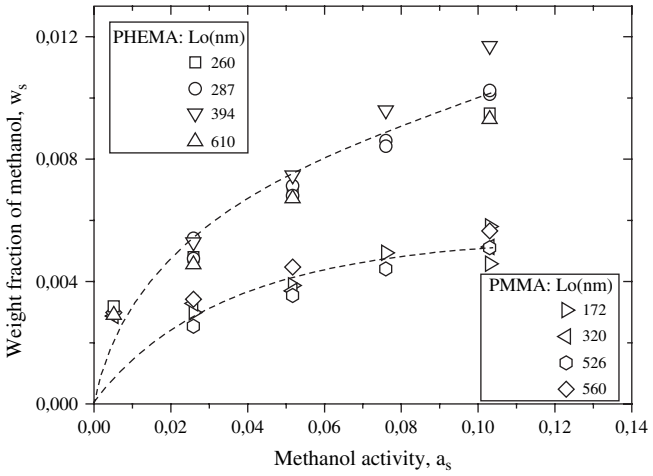

Fig. 4. Sorption isotherm of MeOH vapor in PMMA (lower curve) and PHEMA (upper curve) films, supported on Si/SiO_2 substrate, at 30 °C. The weight fraction of MeOH was calculated from the equilibrium fractional thickness increase $\delta L/L_o$ assuming unidirectional swelling and volume additivity upon mixing. The lines have been drawn to aid the eye.

to $a_s = 0$. A typical example is shown in Fig. 3. From the equilibrium expansion data, the fractional film expansion $\delta L/L_o$ at each activity was determined. Assuming (i) one-directional swelling of the supported film along the thickness direction, i.e. $\delta L/L_o = \delta V/V_o$ and (ii) volume additivity upon mixing, the penetrant uptake per unit mass of dry polymer Q, the weight (w_s) and volume (φ_s) fractions of penetrant in the polymer–penetrant mixture are given by

$$Q(\text{g/g dry pol}) = m_s/m_p = (\delta V/V_o)(d_s/d_p) = (\delta L/L_o)(d_s/d_p) \quad (2)$$

$$w_s = Q/(Q+1) \quad (3)$$

$$\varphi_s = \delta L/(L_o + \delta L_o) \quad (4)$$

where m_s, m_p are the masses of sorbed penetrant and of dry polymer, respectively, and d_s, d_p are the corresponding densities of pure solvent and pure polymer.

3. Results and discussion

3.1. Sorption isotherms

In order to compare the results obtained by the above optical technique with sorption literature data deduced by direct gravimetric methods in bulk, free-standing films, the measured equilibrium expansion $\delta L/L_o$ of relatively thick films ($L_o > 100$ nm) exposed to different activities a_s of the vapor penetrant was used to determine the sorption isotherm of each system, on the basis of the assumptions described in the preceding section.

The resulting isotherms of the PMMA–MeOH and PHEMA–MeOH systems are shown in Fig. 4. For each system, the results obtained from the films of different thicknesses are in satisfactory agreement. In the range of methanol activities studied here, both isotherms show a convex-upward curvature, characteristic of glassy polymer–penetrant systems and commonly associated with adsorption in pre-existing cavities that constitute the excess free volume of a glassy polymer matrix [22,23]. The higher sorptive capacity for MeOH exhibited by PHEMA is attributed to the higher polarity and hydrogen-bonding ability of this polymer as compared to PMMA.

The moisture sorption isotherms for PMMA and PHEMA up to activity (relative humidity) $a_s = 0.6$ are shown in Fig. 5. The water uptake is significantly higher in the more hydrophilic PHEMA, as a result of which the corresponding isotherm tends to show a concave upwards curvature at the high activity region, characteristic of the Flory–Huggins solution behavior. It should be noted that, as in the case of methanol, a free volume hole-filling region may exist in the low activity region of the

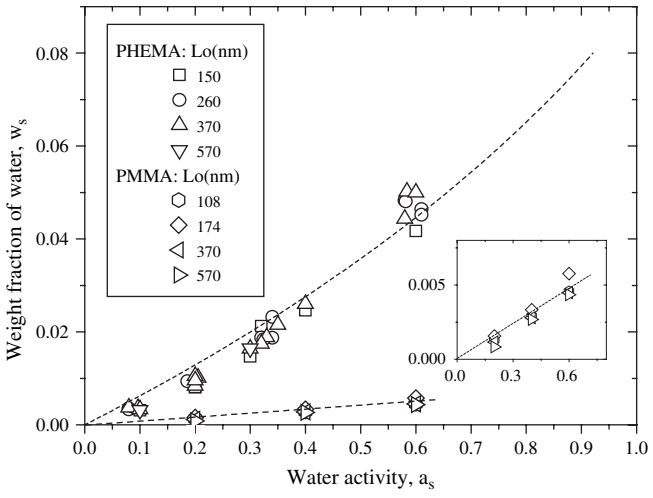

Fig. 5. Sorption isotherm of H_2O vapor in PMMA (lower curve) and PHEMA (upper curve) films, supported on Si/SiO_2 substrate, at 30 °C. The weight fraction of MeOH was calculated from the equilibrium fractional thickness increase $\delta L/L_o$ assuming unidirectional swelling and volume additivity upon mixing. The dashed lines represent the Flory–Huggins isotherms calculated on the basis of Eq. (5) with χ 1.8 (upper curve) and 3.3 (lower curve). The PMMA–H_2O data are shown in greater detail in the inset.

water vapor isotherms, undetectable in the data of Fig. 5 due to the lack of experimental measurements at $a_s < 0.1$.

The shape of the sorption isotherms of Figs. 4 and 5 is in line with those found in literature, by gravimetric methods, for free-standing bulk films. In particular, Connelly et al. [24] as well as Dimos and Sanopoulou [23], have obtained a convex-upward type of isotherm in the PMMA–MeOH system in the low activity region ($a_s < 0.2$) at 35 °C and 25 °C, respectively. Rodriguez et al. [25], as well as Sun and Lee [26], have observed a Flory–Huggins isotherm for moisture absorption in PHEMA at 37 °C. For a quantitative comparison in the case of glassy polymers, one should bear in mind that samples prepared by the same experimental procedure and with the same thermal and sorption histories should be considered. Nevertheless, there is a trend of the estimated penetrant uptakes to be lower in the supported films studied here, especially at higher activities and higher degrees of swelling. In particular, our data on the PMMA–MeOH system compare favorably with those of Connelly et al. [24] up to an activity $a_s \sim 0.05$ but are considerably lower at $a_s = 0.1$. In order to compare our results with those of Rodriguez et al. [25], Flory–Huggins interaction parameter χ, at each activity, was calculated from the experimental data of Fig. 4, on the basis of [27]

$$\ln a_s = \ln \varphi_s + (1 - \varphi_s) + \chi(1 - \varphi_s)^2 \quad (5)$$

The estimated values of χ range from 1.7 to 2.0 for the PHEMA–water system and from 3.8 to 3.9 for the PMMA–water system, to be compared with corresponding values 1.4–1.5 and 3.0–3.3 of Rodriguez et al. The corresponding lower penetrant uptakes, found here for supported films as compared to free-standing ones, have been also observed in other cases [10,11]. Several reasons may be responsible for this discrepancy. It may be the result of an artifact, i.e. failure of the assumption of one-dimensional dilation along the thickness direction, and consequently breakdown of Eqs. (2)–(4), as was shown in a study of methylene chloride vapor in cellulose acetate membranes, concerning higher degrees of swelling of thicker films [11]. Additionally, in the present work, an underestimate of penetrant uptake may also arise from the use of a constant value for the refractive index of the swollen polymer layer, in fitting the experimental spectrum by Eq. (1). Both effects are expected to become more important at high degrees of swelling (e.g. in the case of the PHEMA–H_2O system). There is also the possibility that supported films cannot attain full volume swelling equilibrium, due to the constraints imposed on lateral swelling by the support [11]. This effect is expected to be more important at low degrees of swelling, as for example in the PMMA–H_2O or PMMA–MeOH systems. Finally, it may arise from accelerated, diffusion-controlled, physical aging of thin films, resulting in a lower fractional excess free volume, as shown by the lower Langmuir sorption capacity of supported, 120 nm thick, films as compared to free-standing, 50 μm, ones for CO_2 sorption in a polyimide [10]. On the other hand, what is of main importance here in relation to the information derived by our optical methodology, is that swelling behavior of the systems studied show the same trends with increasing penetrant activity, as those obtained by direct gravimetric sorption methods in bulk free-standing films.

3.2. Effect of polymer film thickness and of substrate

As discussed in Section 1, in the case of relatively hydrophobic polymers supported on hydrophilic substrates, fractional swelling due to moisture absorption, increases with decreasing L_o, due to the accumulation of water near the substrate–polymer interface. Accordingly, from the two polymers studied here, the more hydrophobic PMMA, is likely to exhibit an analogous behavior. The fractional swelling of PMMA films supported on Si/SiO_2 vs the dry film thickness, for three different moisture activities, is shown in Fig. 6. Evidently, for $100 < L_o < 600$ nm, the fractional swelling is independent of film's thickness [in particular, $\delta L/L_o = (1.4 \pm 0.3) \times 10^{-3}$, $(3.2 \pm 0.1) \times 10^{-3}$ and $(5.4 \pm 0.2) \times 10^{-3}$ for $a_s = 0.2$, 0.4 and 0.6, respectively]. The reproducibility of the results becomes less satisfactory as L_o falls below 100 nm due to the considerably lower δL values attained, but a distinct trend of $\delta L/L_o$ to increase with decreasing L_o is observed for all activities, in accordance with expectations.

The corresponding behavior of Si/SiO_2-supported PMMA films exposed to methanol vapor was also studied. As shown in Fig. 7, the opposite trend was observed in this case, i.e. a decreasing fractional swelling with decreasing thickness. In particular, $\delta L/L_o = (7.8 \pm 0.8) \times 10^{-3}$ for 100 nm $< L_o <$ 600 nm, and falls to $(4.0 \pm 0.7) \times 10^{-3}$ for films with 27 nm $< L_o <$ 31 nm. Although methanol is less polar and has a higher affinity for PMMA as compared to water (as shown by the sorption isotherms of Figs. 4 and 5), it is unlikely that the observed behavior is due to the depletion of MeOH near the SiO_2 surface, as was assumed to be the case in the highly hydrophilic PVP–SiO_2–H_2O system [4]. In order to further investigate the phenomenon, we also studied methanol-induced swelling of PMMA films supported on SiO_2 surface treated with HMDS.

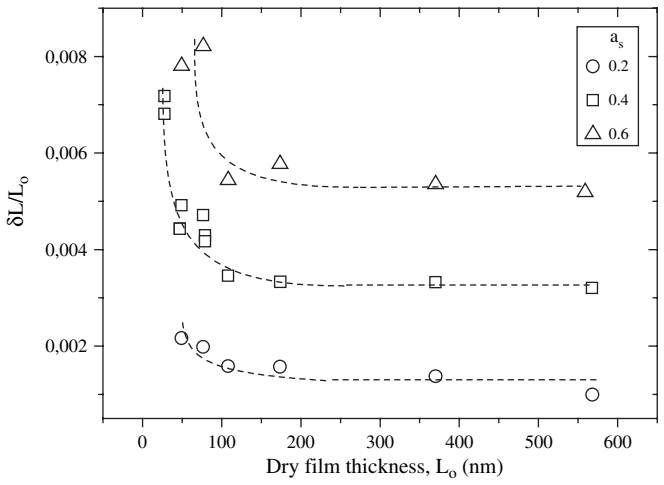

Fig. 6. Fractional thickness expansion vs dry film's thickness, due to water vapor sorption in PMMA films supported on Si/SiO_2 substrate. Results for three different water vapor activities a_s are presented.

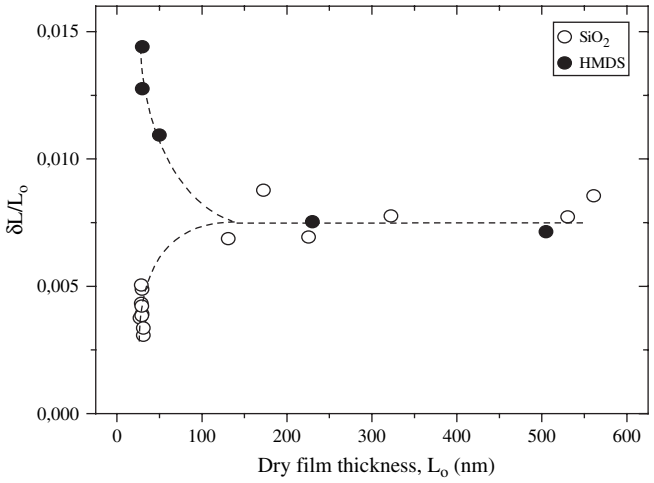

Fig. 7. Fractional thickness expansion vs dry film's thickness, due to methanol vapor sorption in PMMA films supported on bare Si/SiO_2 (○) and HMDS-treated Si/SiO_2 (●) substrate. Activity of MeOH vapor a_s: 0.10.

As shown in Fig. 7, the treatment resulted in fractional swelling increasing with decreasing film thickness L_o. A possible interpretation of the data of Fig. 7, can be based on the respective behavior of the T_g of supported PMMA films, discussed in Section 1. In particular, the experimentally observed T_g enhancement with decreasing L_o for Si/SiO_2-supported PMMA films [12–14] indicates strong polymer–substrate interactions (possibly of hydrogen-bonding type [13]), leading to reduced chain mobility and increased packing density of polymer chains near the buried interface. It is reasonable to assume that the said strong interactions will also lead to strong adhesion, and consequently constrained swelling, of the determinant polymer layer near the substrate. On the other hand, the observed T_g reduction with decreasing L_o for HMDS-treated SiO_2 surfaces [12] point to weak polymer–substrate interactions. In this case, the free surface effect (enhanced mobility and lower packing density) dominates the properties of the ultrathin film. Accordingly, the top layer is expected to exhibit a higher sorptive capacity as compared to the bulk, leading to enhanced fractional swelling with decreasing thickness.

4. Conclusions

The interferometric results on the thickness expansion of supported polymer films, exposed to different activities of the methanol or water vapor, were used to determine the sorption isotherm of the system. Data for relatively thick films ($L_o > 100$ nm) show the same trends with increasing penetrant activity, as those obtained by direct gravimetric sorption methods in bulk free-standing films. On a quantitative basis, the estimated penetrant uptakes, tend to be lower in the supported films studied here, especially at higher activities and higher degrees of swelling, possibly due to the simplifying assumptions used for the derivation of the thickness changes and corresponding mass uptakes, or to actual partial suppression of volume swelling, or to accelerated physical aging.

The results on the thickness dependence of methanol-induced swelling of PMMA films supported on bare, as well as on HMDS-treated Si/SiO_2 substrates indicate that the said behavior of ultrathin polymer films can be correlated to the relevant behavior of the T_g of the polymer.

Acknowledgments

This work has been supported by (a) the Education and Initial Vocational Training Program – Archimedes (project of Athens TEI 2.2-23) funded by E.U. (75%) and by the Greek Government (25%) and (b) a Greek–Polish bilateral cooperation project.

References

[1] Vogt BD, Soles CL, Lee H-J, Lin EK, Wu W. Langmuir 2004;20:1453–8.
[2] Quercia L, Loffredo F, Bombace M, Nasti I, Di Francia G. Sens Actuators B 2005;111–112:166–70.
[3] Huang H, Xu Y, Low HY. Polymer 2005;46:5949–55.
[4] Vogt BD, Soles CL, Lee H-J, Lin EK, Wu W. Polymer 2005;46:1635–42.
[5] Dubreuil AC, Doumenc F, Guerrier B, Allain C. Macromolecules 2003;36:5157–64.
[6] Vogt BD, Soles CL, Jones RL, Wang C-Y, Lin EK, Wu W, et al. Langmuir 2004;20:5285–90.
[7] Vogt BD, Prabhu VM, Soles CL, Satija SK, Lin EK, Wu W. Langmuir 2005;21:2460–4.
[8] Beck Tan NC, Wu WL, Wallace WE, Davis GT. J Polym Sci Part B Polym Phys 1998;36:155–62.
[9] Sirard SM, Green PF, Johnston KP. J Phys Chem 2001;105:766–72.
[10] Wind JD, Sirard SM, Paul DR, Green PF, Johnston KP, Koros WJ. Macromolecules 2003;36:6433–41.
[11] Stamatialis DF, Wessling M, Sanopoulou M, Strathmann H, Petropoulos JH. J Membr Sci 1997;130:75–83.
[12] Fryer DS, Nealy PF, de Pablo JJ. Macromolecules 2000;33:6439–47.
[13] Keddie JL, Jones RAL, Cory RA. Faraday Discuss 1994;98:219–30.
[14] Raptis I, Diakoumakos CD. Microelectron Eng 2002;61–62:829–34.
[15] Fryer DS, Peters RD, Kim EJ, Tomaszewski JE, de Pablo JJ, White CC, et al. Macromolecules 2001;34:5627–34.
[16] Laschitsch AL, Bouchard C, Habicht JH, Schimmel M, Ruhe JR, Johannsmann D. Macromolecules 1999;32:1244–51.
[17] Mattson J, Forrest JA, Borjesson L. Phys Rev E 2000;62:5187–200.
[18] Torres JA, Nealey PF, de Pablo JJ. Phys Rev Lett 2000;85:3221–4.
[19] Van Krevelen DW. Properties of polymers. 3rd ed. Amsterdam: Elsevier Science Publishers; 1990 [chapter 9].
[20] Goustouridis D, Manoli K, Chatzandroulis S, Sanopoulou M, Raptis I. Sens Actuators B 2005;111–112:549–54.
[21] Heavens OS. Optical properties of thin solid films. Dover Publications; 1991.
[22] Toi K, Morrel G, Paul DR. J Appl Polym Sci 1982;27:2997–3005.
[23] Dimos V, Sanopoulou M. J Appl Polym Sci 2005;97:1184–95.
[24] Connelly RW, McCoy NR, Koros WJ, Hopfenberg HB, Steward ME. J Appl Polym Sci 1987;34:703–19.
[25] Rodriguez O, Fornasiero F, Arce A, Radke CJ, Prausnitz JM. Polymer 2003;44:6323–33.
[26] Sun Y-M, Lee H-L. Polymer 1996;37:3915–9.
[27] Flory PJ. Principles of polymer chemistry. London: Cornell University Press; 1953 [chapter XII].